

## Principles of NMDA Receptor Allosteric Modulation

*Author:* Gabriela Popescu

*Institution:* Department of Anesthesiology, Department of Physiology and Biophysics  
and Center for Single Molecule Biophysics, University at Buffalo, Buffalo NY 14214

## Running title: **NMDA receptor modulation**

### *Corresponding author and contact information:*

Dr. Gabriela Popescu

University at Buffalo, Department of Physiology and Biophysics

124 Sherman Hall, 3435 Main Street, Buffalo, NY 14214

Phone: 716-829-3450; Fax: 716-829-2569

E-mail: [popescu@buffalo.edu](mailto:popescu@buffalo.edu)

### *Manuscript statistics:*

Pages (including references and legends): 30

Tables: 2

Figures: 4

References: 39

Abstract: 229 words

Introduction: 749 words

Discussion: 1439 words

### *Abbreviations footnote:*

NMDA, N-methyl-D-aspartate;

NR, N-methyl-D-aspartate receptor

*Abstract:*

NMDA receptors are glutamate-gated ion channels with complex participation in synaptic transmission, integration and plasticity. They are highly permeable to  $\text{Ca}^{2+}$ , activate with characteristic kinetics and generate currents with distinct amplitudes according to stimulation frequency. Multiple endogenous and pharmacological agents bind at distinct locations throughout the protein and modulate NMDA receptor responses with allosteric mechanisms. The NMDA receptor activation pathway consists of a series of consecutive, step-wise structural rearrangements rather than a binary, closed-open reaction. This high-resolution multi-state gating reaction is used here to investigate the effects of ideal, state-specific modulators on physiologically relevant parameters of the macroscopic responses to single-pulse and to high-frequency repetitive stimulation. The simulations suggest three significant aspects of NMDA receptor modulation: 1) modest, one kcal/mol bidirectional perturbations in receptor free energy cause up to a 50-fold change in the total charge transferred; 2) activators modulate primarily response time-course while inhibitors are more effectively modulating current peak amplitude; and 3) state-specific modulators have opposite effects on charge transfer and current potentiation by high-frequency stimulation. Importantly, the results imply that the magnitude of the NMDA receptor-mediated  $\text{Ca}^{2+}$  influx and the receptor's ability to discriminate stimulation frequency can be controlled separately. This report suggests that a detailed mechanistic characterization of NMDA receptor allosteric effectors may identify function-specific modulators and provides a road map for the development of combinatorial strategies for local, transient tuning of specific receptor functions.

*Introduction:*

Glutamate-triggered ionic fluxes through NMDA receptors (NRs) contribute to synaptic transmission, synaptic integration, and bidirectional long-term synaptic plasticity in the central nervous system (McBain and Mayer, 1994; Dingledine et al., 1999). Multiple mechanisms control NR signals. Gene expression, differential splicing, protein targeting and turn-over determine the number, molecular composition and cellular location of NRs. According to brain region, developmental stage and synaptic vs. non-synaptic location, NRs generate currents with signature waveforms (Cull-Candy et al., 2001). In addition, the kinetics of the NR response can be effectively modulated by ligands binding at multiple allosteric sites (Yamakura and Shimoji, 1999).

NRs are under tight allosteric control *in vivo* and represent important pharmacologic targets. Endogenous extracellular ions including  $Zn^{2+}$ ,  $Mg^{2+}$  and  $H^+$  maintain NRs under physiologic tonic inhibition (Mayer et al., 1984; Westbrook and Mayer, 1987; Traynelis and Cull-Candy, 1990). Polyamines, arachidonic acid, neurosteroids, ethanol and nitric oxide, as well as redox and phosphorylation reactions also modify channel activity (Yamakura and Shimoji, 1999; Loftis and Janowsky, 2003). Inappropriate NR activity contributes to severe neuropathologies including acute and chronic neurodegeneration, chronic pain and addiction and mental disorders (Hardingham and Bading, 2003). Still, the promise of NR targeted therapies remains largely unfulfilled due to unacceptable side effects of indiscriminate NR inhibition (Kemp and McKernan, 2002). The development of pharmacologic agents that can suppress harmful NR activities while preserving this receptor's vital functions remains an elusive objective and requires a more in-depth understanding of the principles that govern the allosteric modulation of NR activation.

Allosteric theory postulates that allotropic ligands alter a protein's activity by binding with distinct affinities to resting vs. active receptor conformations, in effect forcing a dynamic redistribution of receptors among the two functionally distinct states (Monod et al., 1965; Changeux and Edelstein, 1998). This conceptual framework describes adequately the allosteric modulation of proteins whose activation follows a two-state isomerisation reaction. However, most receptors visit a larger repertoire of functionally discrete states during activation and state-specific ligands are likely to have correspondingly distinct sets of modulatory effects (Kenakin, 2003). Recently, multi-state kinetic models have been used successfully to describe the activation reactions of two NR isoforms (Banke and Traynelis, 2003; Popescu and Auerbach, 2003). Both schemes account well for the complex patterns of currents observed in single-channel records and for the characteristic waveforms of the ensemble responses. In addition, the detailed description of the NR1/2A activation demonstrated that NR current amplitudes vary according to stimulation frequency (Popescu et al., 2004).

The roles played by NRs at central synapses are complex and incompletely understood. At least three characteristics of the NR ensemble response are of particular interest: 1) the total charge transferred; 2) the current waveform; and 3) its sensitivity to stimulus frequency. Due to NRs' substantial  $\text{Ca}^{2+}$  permeability, the total charge transferred scales directly with the amount of  $\text{Ca}^{2+}$  injected into the post-synaptic cell (Burnashev et al., 1995; Schneggenburger, 1996). Post-synaptic  $\text{Ca}^{2+}$  transients initiate in a concentration-dependent manner, bidirectional plastic changes or may trigger neurodegeneration (Tymianski et al., 1993; Cormier et al., 2001; Ismailov et al., 2004). In turn, the shape of the NR current, which is strongly influenced by its relaxation kinetics sets a temporal window for the effective summation of responses across

multiple synapses and contributes to temporal and spatial integration of synaptic inputs (Carmignoto and Vicini, 1992; Watanabe et al., 1992). Last, the ability of NRs to double their response amplitudes when stimulated with high-frequency pulse trains makes them into veritable frequency discriminators (Popescu et al., 2004). This ability to translate frequency-encoded information into intracellular  $\text{Ca}^{2+}$  amplitudes may be crucial to the NR involvement in long-term plasticity. Explicit correlations between state occupancies, physiologically relevant macroscopic behaviors and biological functions have not yet been described.

To investigate the principles governing the allosteric control of NR functions I have used the multi-state activation scheme to examine correlations between fluctuations in specific rate constants, as elicited by state-specific modulator types, and the physiologically relevant properties of the ensemble current. The results illustrate that distinct response phenotypes are elicited according to the specific kinetic transitions modified by a particular heterotropic effector; suggest that charge transfer is highly sensitive to allosteric modulation and can be regulated without affecting the receptor's sensitivity to stimulus frequency; and predict that fluctuations in a distinct set of rate constants control the receptor's sensitivity to high-frequency stimulation with opposite effects on charge transfer. These novel predictions encourage further characterization of the kinetic mechanisms employed by particular endogenous and pharmacologic NR allosteric modulators with the promise of identifying function-specific agents.

### *Methods:*

All simulations were done in the Simu interface of the QUB kinetic analysis software ([www.qub.buffalo.edu](http://www.qub.buffalo.edu)). Starting with a user specified Markov model (number and conductance properties of states, state connectivities and associated rates for each postulated transition) the program calculates for each channel the most probable sequence of transitions with associated state-occupancy durations. Macroscopic currents are calculated from time-dependent probabilities of occupying conducting states and each state's specified conductance. Control currents from 10,000 channels were simulated with the model and rates in Figure 1a, where the unitary conductance of C states was set at zero and that of O states at 10 pA. This single-channel current amplitude corresponds to NR1/2A channels in cell-attached patches exposed to 150 mM NaCl, 2.5 mM KCl, 10 mM HEPBS buffered at pH8, and driven by +100 mV in the recording pipette. At time zero, all channels populated the resting, unliganded and non-conducting state  $C^U$ . Following the stimulation protocols described below, currents developed in a time-dependent manner mirroring the combined dynamic occupancies of the  $O_1$  and  $O_2$  states. These currents were sampled at 20 kHz.

In this study, state-specific allosteric modulators were defined as ligands that bind preferentially to distinct kinetic states and that alter only one rate constant. The effect of a positive/negative state-specific modulator on channel kinetics was modeled as a 5-fold increase (5x of control) or decrease (0.2x of control) in a specific rate constant, each reflecting a change in receptor free energy of  $\sim 1$  kcal/mol. Activators were considered to increase forward rate constants (toward  $O_2$ ) or decrease backward rate constants (from  $O_2$ ). Conversely, inhibitors were considered to decrease forward rate constants or increase backward rate constants.

Stimulation protocols consisted of either a single pulse or a theta-like burst, which consisted of a train of 5 consecutive pulses with a 10 ms inter-pulse interval (100 Hz), as indicated in the text. Each pulse was approximated as a square step into 1-mM glutamate lasting 1 ms. For each state-specific effector (*i.e.* set of rate constants) and a given stimulation protocol (single-pulse or theta-burst), ten current traces (1 s each) were simulated and averaged for analysis. Time constants for the rise and the relaxation phases of the averaged traces ( $RT$ ,  $\tau_{\text{decay}}$ ) and the maximal current amplitudes ( $I_{\text{peak}}$ ) were determined by fitting each current phase to a single exponential function directly in the QuB program. Open probabilities ( $P_o$ ) were calculated from  $I = nP_o\gamma$ , where  $n$  represents the number of channels and  $\gamma$ , the unitary conductance. Charge transfer was calculated in Origin<sup>®</sup> (Northampton, MA) as the integrated area under the curve of stimulus-evoked current from time zero to 1 s. The simulations described here were done with a large number of channels to reduce fluctuations due to the probabilistic nature of gating transitions however, at most synapses only few (<10) receptors are present therefore, charge transfer was normalized to the number of channels to allow easy comparison with results in the literature.

The activation energy diagram (Fig. 1b) was constructed relative to the ground state  $C_1$ . The free energies of all other states were calculated from the rate constants in Fig. 1a using the relationship  $\Delta G_0 = -RT(\ln K_{\text{eq}})$ , where  $R$  is the molar gas constant,  $T$  is the absolute temperature and  $K_{\text{eq}}$  is the equilibrium constant of the transition considered, calculated as the ratio of the forward to reverse rate constants. Barrier heights were represented as:  $E_n^\ddagger = \Delta G_n^0 + (10 - \ln k_{+n})$ .



*Results:*

Effects on the magnitude and shape of the NR response to single-pulse stimulation.

NRs activate with uniquely slow kinetics which reflect receptor oscillations between several non-conducting conformations prior to reaching active, ion-permeable states. Because the intermediate states leading to open conformations are sufficiently long-lived to be detected with suitable resolution in recordings of single-channel currents, the main kinetic events associated with NR gating have been successfully described with statistical methods (Banke and Traynelis, 2003; Popescu and Auerbach, 2003; Erreger et al., 2004). This approach has demonstrated that the NR activation can be minimally conceptualized as the receptor's serial occupancy of seven energetically and functionally distinct states (Fig. 1). The six receptor transitions describing agonist-binding and receptor gating are characterized by associated pairs of forward/backward rate constants which have been estimated for NR1/2A receptors by fitting this scheme directly to entire sequences of single-channel intervals (Fig. 1a) (Popescu et al., 2004). Using standard thermodynamic relationships, this kinetic description of the NR activation pathway can be translated into relative free-energy fluctuations, thus illustrating the free energy landscape experienced by NRs during activation (Fig. 1b). In functional terms, the NR activation sequence is initiated by glutamate binding to resting, or un-liganded receptor conformations and continues with three successive, step-wise receptor isomerisations. The first conformational change ( $C_1 \rightarrow C_2$ ), which is rate-limiting for both the activation (toward O states) and the deactivation (away from O states) pathways, most likely coincides with a structural rearrangement that results in a change in receptor affinity for glutamate, as indicated by a negligible probability of glutamate dissociating from subsequent receptor states ( $C_{2,3}$  and  $O_{1,2}$ ) (Popescu et al., 2004). The

conformational change represented by the  $C_3 \rightarrow O_1$  transition coincides with a switch in the conductance properties of the receptor, such that a receptor's observable response (ionic flux) will be determined by the combined fractional occupancies of the two ion-permeable states,  $O_1$  and  $O_2$  (Fig.1c).

To determine whether general rules can be inferred that relate changes in individual rate constants with macroscopic receptor behaviors, control currents were simulated from 10,000 channels (10 pA each) with the model and rates illustrated in Figure 1a. To estimate receptor responses in the presence of active concentrations of state-specific positive and negative allosteric modulators, currents elicited by a single pulse were simulated with models in which each rate constant, as identified with the notations in Figure 1c, was in turn, increased or reduced 5-fold. The simulated currents were subsequently analyzed in terms of maximal amplitudes and time constants for the rise and decay phases and of the total charge transferred per channel. The results are illustrated in Figure 2a. The values in Table 1 (single-pulse stimulation) reflect the modulation by a state-specific positive effector ligand, one that increases a forward reaction rate or reduces a reverse one according to the kinetic mechanism employed. Table 2 summarizes results for a negative state-specific effector.

The simulations clearly indicate that *total charge* transferred through NRs following single-pulse stimulation was effectively controlled at all kinetic transitions investigated, except for the association rate constant  $k_+$ , where a 5-fold change (increase or decrease) had no detectable effect on charge transfer. This latter observation was anticipated because the glutamate concentration used (1 mM  $\approx$  300  $K_d$ ) strongly dominated the kinetics of the glutamate association reaction even after a 5-fold change in  $k_+$ . At all other transitions, a 5-fold change in any single rate constant

resulted in ~5-fold changes in the amount of charge transferred. Therefore, charge transfer through NRs was uniformly and effectively controlled at all the kinetic steps investigated. In contrast, the shape of the response varied with the kinetic mechanism employed by the modulator.

The *rise times* for currents driven with a single pulse were fit poorly by single exponentials; were always considerably faster than the decay times; and varied only modestly (~2-fold) with a 5-fold change in any rate constant in the model (Tables 1 and 2). Thus, the simulations indicate that the major contributors to the large changes in charge transfer observed were due to changes in peak open probability (peak  $P_o$ ) and decay kinetics ( $\tau_{\text{decay}}$ ).

Overall, activators increased charge transfer by inducing responses with longer relaxation times whereas decreases in charge transfer prompted by inhibitors reflected primarily the lower amplitudes of such responses (Fig. 2a, b). Thus, activators and inhibitors, even when equally effective in controlling charge transfer, had distinct effects on the shape of the NR current. In particular, changes in the kinetics of the first receptor isomerisation reaction ( $C_1 \leftrightarrow C_2$ ) affected differentially the current's decay and amplitude. For a similar change in charge transfer, a decrease in the forward rate  $k_{+1}$ , modeling the action of a negative modulator, resulted in currents with 4-fold lower amplitudes but only 2-fold faster decay kinetics. In contrast, a decrease in  $k_{-1}$ , which simulated the action of a positive effector, resulted in currents with >4-fold longer  $\tau_{\text{decay}}$  and only 2-fold higher amplitudes (Fig. 2b). The relative resistance of rise and decay times to being accelerated suggest that the NR reaction mechanism has a built-in limit to how much a single state-specific modulator can shorten the activation time.

To investigate the sensitivity of NR deactivation time-course to modulation, currents were simulated with models where the rate-limiting step in the deactivation pathway, the dissociation rate constant  $k$ , was varied over four orders of magnitude. Results show that although decay time constants vary steeply for  $k$  values that are slower than controls (*i.e.* activator modulation), the effect of a single state-specific negative modulator on NR1/2A current decay is limited by the reaction mechanism (Fig. 2c). The limitation stems from a deactivation pathway in which two separate transitions have comparably slow, potentially rate-limiting kinetics: the glutamate dissociation step represented by  $k$  and the receptor structural rearrangement represented by  $k_1$ . In effect, this intrinsic kinetic arrangement ensures that a perturbation that increases only *one* of these two rate constants will have minimal effect on  $\tau_{\text{decay}}$ . In contrast, there was no apparent limit to how much the current decay phase of NR1/2A receptors could be extended (Fig. 2c). A similar mechanism appears to limit the effects of a single rate-specific activator on receptor rise time, perhaps acting to preserve the characteristic slow activation of these receptors. In summary, these simulations suggest that the NR gating machinery contains intrinsic rate-stabilizing components.

#### Effects on responses to pulse trains

NR1/2A receptors generate currents with distinct amplitudes according to the frequency of the glutamate pulses with which they are stimulated. In response to a single pulse, NRs generate currents with half-maximal amplitudes; a second pulse arriving at a 10-ms interval (100 Hz) increases the response amplitude (Popescu et al., 2004). It has been suggested that at central excitatory synapses, this so far unique receptor behavior serves to translate the information encoded in the frequency of the incoming electrical pulses into distinct post-synaptic  $\text{Ca}^{2+}$  transients. Since both the frequency of synaptic

discharge and the post-synaptic  $\text{Ca}^{2+}$  concentration carry pertinent information to synaptic physiology, the ability of NRs to, in effect, act as frequency-to-amplitude converters is likely to be the target of physiologically critical regulatory mechanisms.

To determine how many pulses in a high-frequency train are necessary to elicit currents with maximal amplitudes, activity was simulated (10,000 channels, 10 pA) in response to trains of 2-10 pulses (100 Hz) with the model and rates in Figure 1a. Irrespective of the model used, a theta-like burst consisting of 4-6 high-frequency pulses was sufficient to elicit responses of maximal amplitude (data not shown). This high-frequency stimulation protocol was used further in this study. Theta burst-elicited currents had similar rise and decay kinetics as those elicited with a single-pulse protocol. This observation suggests that single pulse- and theta burst-elicited NR responses differ mainly in the amount of charge transferred as dictated by current amplitudes.

To examine possible effects of allosteric modulators on the ability of NRs to vary the amount of charge transferred according to the stimulation protocol, theta burst-induced currents were simulated with the model in Figure 1a and with models where rates were modified, in turn, 5-fold to mimic the action of individual state-specific modulators. Responses were then compared to the corresponding currents elicited by single-pulse stimulation in terms of peak open probabilities and amount of charge transferred per channel (Tables 1 and 2, theta-burst stimulation). The results were counterintuitive: inhibitors increased the receptor's ability to respond differentially to theta-burst stimulation, whereas activators strongly reduced this ability. These behaviors are illustrated in Figure 3a. Fluctuations in glutamate dissociation kinetics ( $k$ ) and the kinetics of the  $\text{C}_1 \leftrightarrow \text{C}_2$  transitions ( $k_{\pm 1}$ ) emerged as the most effective in

controlling the NRs' ability to discriminate stimulus frequency (Fig. 3b). Even for the modest, single rate constant changes employed in this study, negative modulators affecting these particular transitions more than doubled the ratio of theta-burst to single-pulse charge transfer per channel (from 2.4 for control to 5.5 for changes in  $k_{-1}$ ); on the other hand positive effectors virtually eliminated the ability of NRs to respond differentially to theta-burst-stimulation (ratio of theta-burst to single-pulse charge transfer per channel is 1.3 and 1.5 for changes in  $k$  and  $k_{+1}$ , respectively). These results suggest that the NR ability to discriminate stimulation frequency is sensitive to allosteric modulation and that this property is controlled by a subset of NR effectors only. Thus, the relative insensitivity of the frequency-dependent differential charge transfer to variations in the  $k_{\pm 2}$ ,  $k_{\pm 3}$  and  $k_{\pm 4}$  rate constants suggests that allosteric effectors that modify these NR transitions will effectively influence charge transfer but will leave intact the receptor's frequency discrimination properties.

## Discussion

The principles that govern the allosteric regulation of NR activity were systematically investigated *in silico* by examining the effects of modest bi-directional fluctuations in individual microscopic rate constants on the observable parameters of the ensemble responses. Results show that response amplitude, decay time-course and frequency-discrimination are differentially impacted by changes in individual rate constants according to the identity of the kinetic transition affected.

NR-mediated charge transfer was highly sensitive to allosteric modulation. Charge transfer in response to a single pulse was efficiently and uniformly modulated by fluctuations in any one rate constant except for the glutamate association rate constant. A modest 1 kcal variation in receptor state free energy elicited up to 50-fold change in the amount of charge transferred, with ~5-fold bi-directional change following single-pulse stimulation and an additional ~2-fold increase following a high-frequency train. Because NRs have high unitary conductance (Stern et al., 1992) and high  $\text{Ca}^{2+}$  permeability (Jahr and Stevens, 1993; Burnashev et al., 1995; Schneggenburger, 1996), modest fluctuations in receptor gating translate into substantial fluctuations in  $\text{Ca}^{2+}$  influx.

NR-mediated  $\text{Ca}^{2+}$  influx is a salient biochemical signal for the post synaptic cell. In particular, at excitatory synapses onto spiny neurons where free  $\text{Ca}^{2+}$  diffusion is restricted to the minute volumes of dendritic spines, allosteric NR modulation may result in substantial changes in intracellular  $\text{Ca}^{2+}$  concentration even when only few synaptic receptors are expressed (Nimchinsky et al., 2004). This observation may have important implications for neurophysiology and neuropathology alike. Distinct physiologic levels of intracellular  $\text{Ca}^{2+}$  concentrations determine whether a synapse will

be strengthened or weakened in response to synaptic activity, whereas sustained, pathologically high levels of  $\text{Ca}^{2+}$  trigger apoptotic cascades responsible for excitotoxic neurodegeneration (Mody and MacDonald, 1995; Sattler et al., 1998; Cormier et al., 2001; Ismailov et al., 2004). The striking sensitivity to allosteric modulation exhibited by NRs suggested by these simulations raises the possibility that NR allosteric effectors may wield powerful control over NR-dependent post-synaptic physiologic and pathologic phenomena. Agents that modify charge transfer but preserve the receptor's ability to discriminate stimulus frequency may represent better-tolerated pharmacologic interventions.

Activators and inhibitors had distinct effects on the shape of the NR current. For changes in charge transfer of similar magnitude, activators extended the deactivation phase of the response up to 4-fold whereas inhibitors had a lesser (~2-fold) effect. This result correlated with the observation that there was a limit to how fast currents decayed following changes in a single rate constant. NR current decay time is a parameter of particular relevance to several important neuronal functions. It sets the time frame within which activity at neighboring synapses will be integrated; participates in the generation of dendritic spikes; contributes to supra-linear summation of excitatory post-synaptic currents; and sets the temporal window within which synaptic discharge and depolarization in the post-synaptic dendrite are detected as coincidental (Magee, 2000; Schiller et al., 2000; Schiller and Schiller, 2001). NR current decay time is developmentally and regionally regulated by differential expression and dynamic sub-cellular targeting of NRs with distinct subunit compositions (Carmignoto and Vicini, 1992; Watanabe et al., 1992). Allosteric modulation may represent an additional, fast, reversible and perhaps local mechanism to adjust the NR current decay time.



The results presented here suggest that, at least for NR1/2A isoforms, current decay time is resistant to further decrease by allosteric inhibitors but can be easily increased by positive modulators. Interestingly, the NR1/2A receptor is the isoform with the fastest decay kinetics (Vicini et al., 1998). Its apparent resistance to further acceleration suggests that these receptors may serve to set the shortest time frame within which synaptic activity will be integrated.

A single theta-like burst stimulus was sufficient to trigger maximal current amplitude (and thus maximal charge transfer) from NR1/2A receptors. The implication that NRs recognize and respond distinctly to a physiologically occurring electrical pattern may be directly relevant to the roles played by NRs in higher brain functions. Many neurons in the CNS have the ability to generate short bursts of action potentials consisting of 4-6 pulses at 100-200 Hz which repeat with a 200-ms periodicity. This rhythmic activity pattern known as theta rhythm is prevalent in the hippocampus where entire populations of cells fire synchronously with this frequency. In this brain region, theta oscillations have been ascribed a role in cellular plasticity and behavioral learning processes (Berry and Seager, 2001). More specifically, it has been demonstrated *in vitro* that cholinergic induced theta-like activity increases NR-dependent plasticity phenomena (Huerta and Lisman, 1996). In this context, NR inhibition may represent means to enhance NR sensitivity to theta-burst stimulation while tuning-out low-frequency signals.

Notably, current potentiation by high-frequency stimulation was differentially affected by fluctuations in individual rate constants. The most effective control points were the  $k_{-}$  and  $k_{+1}$  rate constants and these had opposite effects on frequency discrimination and charge transfer (Fig.4). Importantly, in most systems stimulation

frequency determines the direction of the ensuing activity-dependent synaptic modification, with high-frequency stimulation (100 Hz) resulting in long-term potentiation and tonic, low-frequency stimulation (1-10 Hz) initiating long-term depression (Herron et al., 1986; Dudek and Bear, 1993). Thus, it is highly plausible that NRs are the molecular transducers which translate patterns of neurotransmitter release into distinct levels of intracellular  $\text{Ca}^{2+}$  to trigger differential plasticity. The simulations presented in this study suggest that allosteric modulators can intervene to increase or annihilate a frequency-dependent differential  $\text{Ca}^{2+}$  influx and thus control how the cell will respond to a particular stimulation frequency. Thus NR allosteric modulators may contribute to physiologic mechanisms for differential synaptic transmission (Markram et al., 1998).

Several limitations inherent to this study need to be stated. This first systematic examination of correlations between state-specific modulators and characteristic behaviors of ensemble NR responses was made possible by the recent high-resolution characterization of the NR1/2A activation reaction; necessarily, the results are limited to this receptor isoform. In addition, although the model captures most recognizable NR physiologic behaviors it is still incomplete as it lacks explicit association/dissociation transitions for the co-agonist glycine and desensitization steps. NR1/2A receptors have remarkably low desensitization and thus it is likely that excluding this latter kinetic component will not greatly affect the results presented here. Still, both the glycine-binding and the desensitization reactions may represent physiologic targets for NR modulation and should be addressed in the future. Lastly, only the effects of 'ideal' modulators, *i.e.* those that affect the rate constant for a single conformational transition were investigated here. In reality, the action of a particular modulator may result in changes in a set of rate constants (see below).

The inhibitory effects demonstrated for calmodulin on NRs native to hippocampal granule cells illustrate several aspects of NR modulation highlighted by the present study. First, it was estimated that calmodulin decreases the amount of charge transferred by a single receptor ~3-fold (from 69 to 23 fC) (Rycroft and Gibb, 2002). Despite differences in the preparation investigated (native vs. recombinant) and experimental conditions (*i.e.* ionic concentrations, pH and membrane potential) these values are remarkably similar to the ones estimated here for ideal inhibitors, *i.e.* 118 (control) to 36-21 fC or ~5-fold decrease. First, this comparison between experiment and simulation indicates that the small free-energy fluctuations assumed in this study are within the range of receptor free energy fluctuations induced by a physiologic modulator. Second, when the effects of calmodulin on NR activity were modeled with a two-state gating scheme, it was found that calmodulin changed the NR opening rate ~7-fold, the channel closing rate ~2-fold and the desensitization rate ~2-fold (Rycroft and Gibb, 2002). Although these estimated opening and closing “rates” amalgamate several microscopic rate constants, it is clear that calmodulin-binding to NRs changes the kinetics of *several* NR transitions, whose integrated effects result in a unique macroscopic phenotype: decreased open probability and increased current decay rate. Last, the effects of calmodulin or any other NR modulator on NR’s frequency discrimination properties have not been yet investigated. The simulations presented here demonstrate that it is critical to determine specifically which microscopic rate constants are affected by a modulator in order to evaluate a modulator’s impact on NR’s sensitivity to stimulus frequency. The predictions afforded by a known kinetic mechanism would help design targeted experimental paradigms to further investigate such effects.

The systematic correlations delineated here between fluctuations in specific microscopic rate constants and physiologically relevant kinetic properties of the macroscopic response provide a theoretical foundation to the search for function-specific modulators; make a strong case for undertaking a detailed characterization of the kinetic mechanisms employed by endogenous and pharmacologic allosteric modulators; and offer a clear road map for combinatorial approaches to the rational control of NR functions. The goal is to be able to predict NR responses in the simultaneous presence of several modulators, as is the case *in vivo*, and the effect of pharmacologic agents on NRs operating in particular physiologic or pathologic conditions.

*Acknowledgements:*

I am indebted to Drs. Tony Auerbach and Mark Lema for outstanding mentorship and for support during the final stages of this project; Chris Nicolai and John Bannen for programming necessary functions into QUB; and Drs. Dan Kosman and Terry Kenakin for valuable comments on the manuscript.

*References:*

- Banke TG and Traynelis SF (2003) Activation of NR1/NR2B NMDA receptors. *Nat Neurosci* 6:144-152.
- Berry SD and Seager MA (2001) Hippocampal Theta Oscillations and Classical Conditioning. *Neurobiology of Learning and Memory* 76:298-313.
- Burnashev N, Zhou Z, Neher E and Sakmann B (1995) Fractional calcium currents through recombinant GluR channels of the NMDA, AMPA and kainate receptor subtypes. *J Physiol* 485 (Pt 2):403-418.
- Carmignoto G and Vicini S (1992) Activity-dependent decrease in NMDA receptor responses during development of the visual cortex. *Science* 258:1007-1011.
- Changeux J-P and Edelman SJ (1998) Allosteric Receptors after 30 Years. *Neuron* 21:959-980.
- Cormier RJ, Greenwood AC and Connor JA (2001) Bidirectional Synaptic Plasticity Correlated With the Magnitude of Dendritic Calcium Transients Above a Threshold. *J Neurophysiol* 85:399-406.
- Cull-Candy S, Brickley S and Farrant M (2001) NMDA receptor subunits: diversity, development and disease. *Curr Opin Neurobiol* 11:327-335.
- Dingledine R, Borges K, Bowie D and Traynelis SF (1999) The glutamate receptor ion channels. *Pharmacol Rev* 51:7-61.
- Dudek SM and Bear MF (1993) Bidirectional long-term modification of synaptic effectiveness in the adult and immature hippocampus. *J Neurosci* 13:2910-2918.
- Erreger K, Chen PE, Wyllie DJ and Traynelis SF (2004) Glutamate receptor gating. *Crit Rev Neurobiol* 16:187-224.

- Hardingham GE and Bading H (2003) The Yin and Yang of NMDA receptor signalling. *Trends Neurosci* 26:81-89.
- Herron CE, Lester RA, Coan EJ and Collingridge GL (1986) Frequency-dependent involvement of NMDA receptors in the hippocampus: a novel synaptic mechanism. *Nature* 322:265-268.
- Huerta PT and Lisman JE (1996) Synaptic plasticity during the cholinergic theta-frequency oscillation in vitro. *Hippocampus* 6:58-61.
- Ismailov I, Kalikulov D, Inoue T and Friedlander MJ (2004) The Kinetic Profile of Intracellular Calcium Predicts Long-Term Potentiation and Long-Term Depression. *J. Neurosci.* 24:9847-9861.
- Jahr CE and Stevens CF (1993) Calcium permeability of the N-methyl-D-aspartate receptor channel in hippocampal neurons in culture. *Proc Natl Acad Sci U S A* 90:11573-11577.
- Kemp JA and McKernan RM (2002) NMDA receptor pathways as drug targets. *Nat Neurosci* 5 Suppl:1039-1042.
- Kenakin T (2003) Ligand-selective receptor conformations revisited: the promise and the problem. *Trends in Pharmacological Sciences* 24:346-354.
- Loftis JM and Janowsky A (2003) The N-methyl-D-aspartate receptor subunit NR2B: localization, functional properties, regulation, and clinical implications. *Pharmacol Ther* 97:55-85.
- Magee JC (2000) Dendritic integration of excitatory synaptic input. *Nat Rev Neurosci* 1:181-190.
- Markram H, Wang Y and Tsodyks M (1998) Differential signaling via the same axon of neocortical pyramidal neurons. *PNAS* 95:5323-5328.

- Mayer ML, Westbrook GL and Guthrie PB (1984) Voltage-dependent block by Mg<sup>2+</sup> of NMDA responses in spinal cord neurones. *Nature* 309:261-263.
- McBain CJ and Mayer ML (1994) N-methyl-D-aspartic acid receptor structure and function. *Physiol Rev* 74:723-760.
- Mody I and MacDonald JF (1995) NMDA receptor-dependent excitotoxicity: the role of intracellular Ca<sup>2+</sup> release. *Trends Pharmacol Sci* 16:356-359.
- Monod J, Wyman J and Changeux JP (1965) On the Nature of Allosteric Transitions: A Plausible Model. *J Mol Biol* 12:88-118.
- Nimchinsky EA, Yasuda R, Oertner TG and Svoboda K (2004) The number of glutamate receptors opened by synaptic stimulation in single hippocampal spines. *J Neurosci* 24:2054-2064.
- Popescu G and Auerbach A (2003) Modal gating of NMDA receptors and the shape of their synaptic response. *Nat Neurosci* 6:476-483.
- Popescu G, Robert A, Howe JR and Auerbach A (2004) Reaction mechanism determines NMDA receptor response to repetitive stimulation. *Nature* 430:790-793.
- Rycroft BK and Gibb AJ (2002) Direct effects of calmodulin on NMDA receptor single-channel gating in rat hippocampal granule cells. *J Neurosci* 22:8860-8868.
- Sattler R, Charlton MP, Hafner M and Tymianski M (1998) Distinct influx pathways, not calcium load, determine neuronal vulnerability to calcium neurotoxicity. *J Neurochem* 71:2349-2364.
- Schiller J, Major G, Koester HJ and Schiller Y (2000) NMDA spikes in basal dendrites of cortical pyramidal neurons. *Nature* 404:285-289.
- Schiller J and Schiller Y (2001) NMDA receptor-mediated dendritic spikes and coincident signal amplification. *Current Opinion in Neurobiology* 11:343-348.



- Schneggenburger R (1996) Simultaneous measurement of Ca<sup>2+</sup> influx and reversal potentials in recombinant N-methyl-D-aspartate receptor channels. *Biophys J* 70:2165-2174.
- Stern P, Behe P, Schoepfer R and Colquhoun D (1992) Single-channel conductances of NMDA receptors expressed from cloned cDNAs: comparison with native receptors. *Proc R Soc Lond B Biol Sci* 250:271-277.
- Traynelis SF and Cull-Candy SG (1990) Proton inhibition of N-methyl-D-aspartate receptors in cerebellar neurons. *Nature* 345:347-350.
- Tymianski M, Charlton MP, Carlen PL and Tator CH (1993) Source specificity of early calcium neurotoxicity in cultured embryonic spinal neurons. *The Journal Of Neuroscience: The Official Journal Of The Society For Neuroscience* 13:2085-2104.
- Vicini S, Wang JF, Li JH, Zhu WJ, Wang YH, Luo JH, Wolfe BB and Grayson DR (1998) Functional and pharmacological differences between recombinant N-methyl-D-aspartate receptors. *J Neurophysiol* 79:555-566.
- Watanabe M, Inoue Y, Sakimura K and Mishina M (1992) Developmental changes in distribution of NMDA receptor channel subunit mRNAs. *Neuroreport* 3:1138-1140.
- Westbrook GL and Mayer ML (1987) Micromolar concentrations of Zn<sup>2+</sup> antagonize NMDA and GABA responses of hippocampal neurons. *Nature* 328:640-643.
- Yamakura T and Shimoji K (1999) Subunit- and site-specific pharmacology of the NMDA receptor channel. *Prog Neurobiol* 59:279-298.

*Footnotes*

This work was supported in part by funds from the National Institutes of Health (DA015164) and the American Heart Association (0535268N).

*Legends for Figures:*

**Figure 1** NR reaction mechanism. **a)** Minimal kinetic scheme proposed for the activation of NR1/2A receptors (reproduced from (Popescu et al., 2004)). All rates are in  $s^{-1}$ , except for  $k_+$ , which is in  $mM^{-1}s^{-1}$ . **b)** Free energy diagram calculated from the rates in a) and a glutamate concentration,  $[G] = 1$  mM. Conformational transitions associated with gating ( $C_1 \leftrightarrow O_2$ ) proceed along a relatively low-barrier, flat free-energy landscape. **c)** Functional correlates of kinetically defined transitions. Distinct kinetic states also differ with respect to: glutamate occupancy ( $C^U$ , unliganded,  $C^M$ , mono-liganded,  $C_{1-3}$  and  $O_{1-2}$ , fully liganded); glutamate affinity ( $C^U$ ,  $C^M$ ,  $C_1$  have measurable affinity:  $K_d = k/k_+$ , whereas glutamate dissociation is statistically negligible from  $C_{2,3}$  and  $O_{1,2}$  states); and ionic permeability (C, non-conducting, O, conducting).

**Figure 2** Modulation of NR responses to single-pulse stimulation. **a)** For a similar ~5-fold change in charge transfer, activators have more pronounced effects on decay kinetics whereas inhibitors more readily change current amplitudes; \*, these effects are illustrated in b). **b)** Current amplitude is most effectively controlled by decreasing  $k_{+1}$  (glutamate trapping); decay time is most markedly modified by decreasing  $k_{-1}$  (glutamate dissociation). **c)** Decay time constants vary steeply with  $k_{-1}$  until they reach a lower limit at  $\sim 20s^{-1}$ .

**Figure 3** Modulation of NR current potentiation by theta-burst stimulation. **a)** Responses to a single pulse (black line) and to a theta-like burst (grey line). Increasing  $k_{+1}$  increases total charge transfer and eliminates theta burst-elicited potentiation. In contrast, reducing  $k_{+1}$  amplifies theta-burst-induced potentiation while reducing charge transfer,  $r$ , ratio of single pulse- to theta burst-elicited charge transfer per channel. **b)**

Activators (white bars) reduce and inhibitors (grey bars) increase theta burst-dependent potentiation. The magnitude of the effect is state-specific.

**Figure 4** Principles of NR allosteric modulation. Charge transfer is uniformly and effectively modulated by changing the rate constant for any conformational transition. The ability of NRs to respond with increased amplitude to theta burst-stimulation is modulated in opposite direction by fluctuations in a specific subset of rate constants (dashed squares).

Tables

**Table 1** Effects of positive modulators on macroscopic properties of NR responses according to the kinetic mechanism employed

| rate<br>(s <sup>-1</sup> ) |       | single-pulse stimulation |                        |                            |                | theta-burst stimulation |                            |                | charge<br>ratio<br>TB/SP |
|----------------------------|-------|--------------------------|------------------------|----------------------------|----------------|-------------------------|----------------------------|----------------|--------------------------|
|                            |       | rise time<br>(ms)        | peak<br>P <sub>o</sub> | τ <sub>decay</sub><br>(ms) | charge<br>(fC) | peak<br>P <sub>o</sub>  | τ <sub>decay</sub><br>(ms) | charge<br>(fC) |                          |
| control*                   |       | 8.8                      | 0.2                    | 47                         | 120            | 0.35                    | 47                         | 275            | 2.3                      |
| k <sub>+</sub>             | 85    | 10.1                     | 0.19                   | 45                         | 110            | 0.35                    | 45                         | 272            | 2.5                      |
| k <sub>+1</sub>            | 600   | 5.1                      | 0.42                   | 120                        | 550            | 0.52                    | 111                        | 800            | 1.5                      |
| k <sub>+2</sub>            | 2900  | 6.3                      | 0.37                   | 145                        | 590            | 0.66                    | 140                        | 1114           | 1.9                      |
| k <sub>+3</sub>            | 12500 | 8.3                      | 0.38                   | 140                        | 590            | 0.7                     | 139                        | 1185           | 2.0                      |
| k <sub>+4</sub>            | 17250 | 11.4                     | 0.33                   | 133                        | 490            | 0.68                    | 132                        | 1053           | 2.1                      |
| k <sub>.</sub>             | 12    | 10.9                     | 0.3                    | 150                        | 510            | 0.38                    | 147                        | 683            | 1.3                      |
| k <sub>-1</sub>            | 32    | 10.5                     | 0.28                   | 192                        | 510            | 0.49                    | 186                        | 1019           | 2.0                      |
| k <sub>-2</sub>            | 522   | 8.5                      | 0.33                   | 150                        | 530            | 0.64                    | 148                        | 1133           | 2.1                      |
| k <sub>-3</sub>            | 432   | 11.7                     | 0.34                   | 155                        | 570            | 0.71                    | 171                        | 1393           | 2.4                      |
| k <sub>-4</sub>            | 132   | 11                       | 0.32                   | 135                        | 500            | 0.67                    | 167                        | 1270           | 2.5                      |

\* See Figure 1a for control values for all rate constants.

**Table 2** Effects of negative modulators on kinetic parameters of NR macroscopic response according to the kinetic mechanism employed

| rate<br>(s <sup>-1</sup> ) |       | single-pulse stimulation |                        |                               |                | theta-burst stimulation |                               |                 | charge<br>ratio<br>TB/SP |
|----------------------------|-------|--------------------------|------------------------|-------------------------------|----------------|-------------------------|-------------------------------|-----------------|--------------------------|
|                            |       | rise time<br>(ms)        | peak<br>P <sub>o</sub> | $\tau_{\text{decay}}$<br>(ms) | charge<br>(fC) | peak<br>P <sub>o</sub>  | $\tau_{\text{decay}}$<br>(ms) | charge<br>(fCl) |                          |
| control                    |       | 8.8                      | 0.2                    | 47                            | 118            | 0.35                    | 47                            | 278             | 2.4                      |
| $k_+$                      | 3.4   | 6.6                      | 0.2                    | 45                            | 121            | 0.35                    | 48                            | 286             | 2.4                      |
| $k_{+1}$                   | 24    | 10.9                     | 0.05                   | 29                            | 21             | 0.12                    | 33                            | 75              | 3.6                      |
| $k_{+2}$                   | 116   | 12.5                     | 0.06                   | 27                            | 23             | 0.11                    | 30                            | 62              | 2.7                      |
| $k_{+3}$                   | 500   | 14.5                     | 0.06                   | 29                            | 23             | 0.09                    | 28                            | 61              | 2.7                      |
| $k_{+4}$                   | 690   | 8.9                      | 0.09                   | 29                            | 36             | 0.14                    | 30                            | 99              | 2.8                      |
| $k_-$                      | 300   | 8.9                      | 0.09                   | 28                            | 33             | 0.21                    | 28                            | 181             | 5.5                      |
| $k_{-1}$                   | 800   | 8.1                      | 0.09                   | 21                            | 21             | 0.13                    | 19                            | 70              | 3.3                      |
| $k_{-2}$                   | 13050 | 9.7                      | 0.06                   | 25                            | 22             | 0.11                    | 25                            | 62              | 2.8                      |
| $k_{-3}$                   | 10800 | 9.7                      | 0.06                   | 26                            | 21             | 0.09                    | 25                            | 61              | 2.9                      |
| $k_{-4}$                   | 3300  | 9.3                      | 0.1                    | 29                            | 37             | 0.13                    | 28                            | 98              | 2.6                      |

\* See Figure 1a for control values for all rate constants.

**Figure 1**

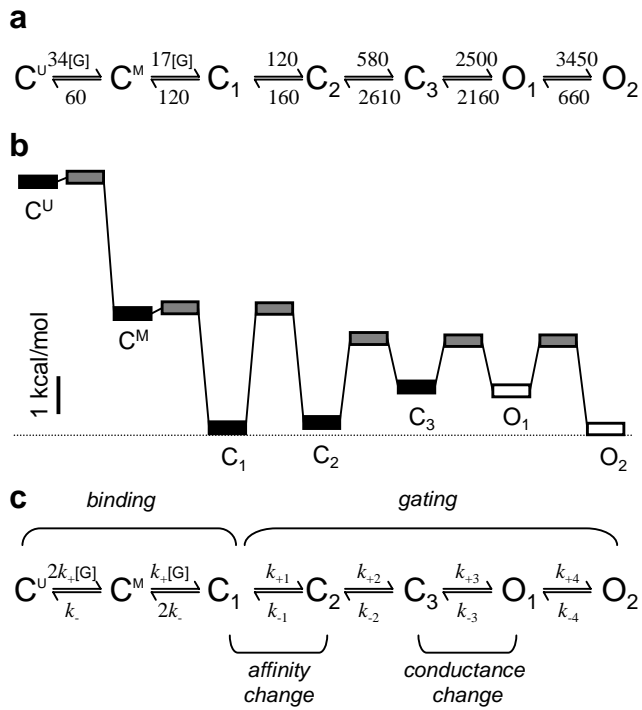


**Figure 2**

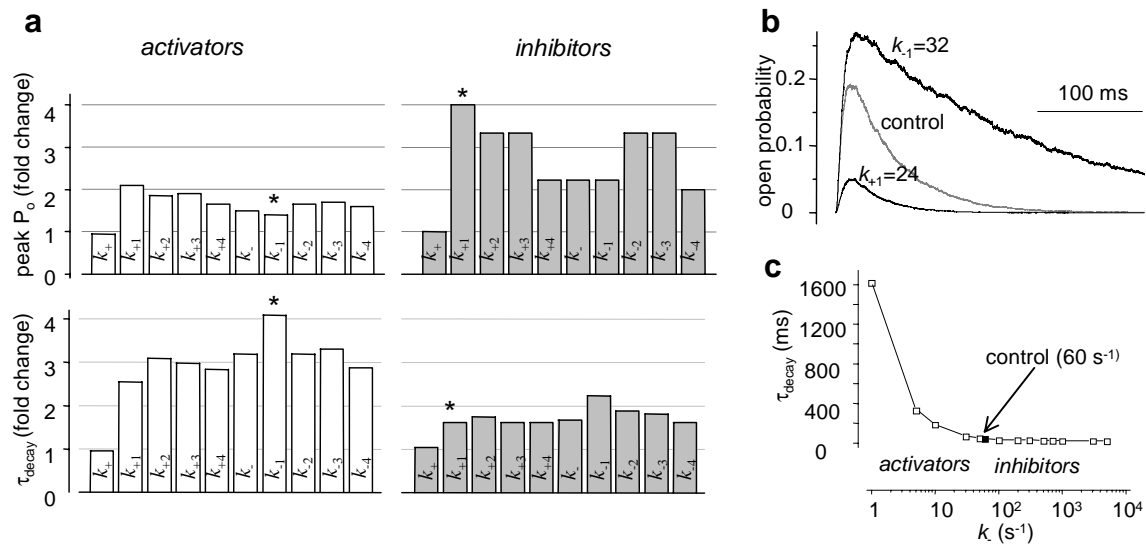




**Figure 3**

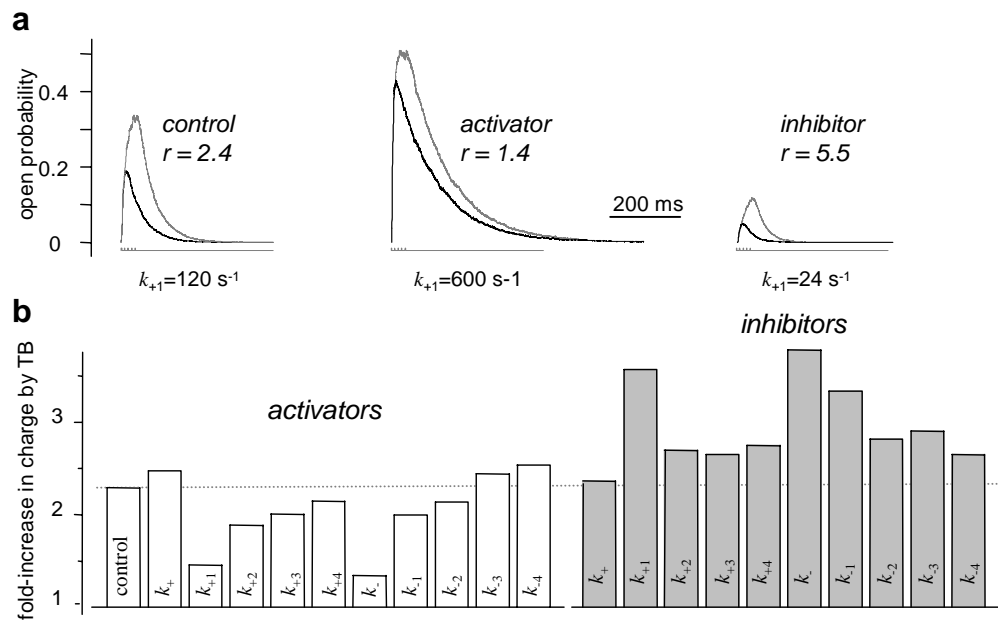


Figure 4

